Azimuthal Fourier Coefficient Elastic Inversion

Benjamin Roure*, Hampson-Russell Software & Services, a CGGVeritas Company, Calgary, Canada
Benjamin.Roure@cggveritas.com
and
Jon Downton, Hampson-Russell Software & Services, a CGGVeritas Company, Calgary, Canada

GeoConvention 2012:Vision

Summary

The benefits of using azimuthal Fourier Coefficients to estimate fracture properties has been proven theoretically and illustrated on real dataset. The 2nd Fourier Coefficient provides a biased estimate of the anisotropic gradient but using a combination of Fourier Coefficients removes that bias, along with estimating an unambiguous symmetry axis. The azimuthal elastic inversion can be modified to invert Fourier Coefficients rather than azimuthal angle stacks in order to estimate fracture parameters. The main advantage of using this alternative data space is to reduce the cross-talk between the fracture and isotropic background parameters. For quality control purpose, the results obtained from the azimuthal elastic inversion can be easily transformed to the anisotropic gradient for comparison with other methods such as the near offset Rüger equation or other reflectivity approaches and these comparisons are illustrated on real dataset. The azimuthal elastic inversion provides layer properties that are easier to relate to the geology than interface properties.

Introduction

The azimuthal elastic inversion of Downton and Roure (2010) extends the simultaneous inversion of Coulon et al. (2006) to not only invert for isotropic parameters but also fracture parameters. This extra information is a consequence of analyzing the azimuthal data which is input as azimuth and angle stacks. The azimuthal elastic inversion uses linear slip deformation theory (Schoenberg, 1980) to model the fractures in a background isotropic earth. The resulting outputs of this inversion are the isotropic parameters (i.e. background density, P-wave and S-wave Impedances) and fracture parameters described in terms of the normal and tangential weaknesses plus the strike of these fractures. The fracture parameter estimates are layer properties and have physical meaning making them easier to interpret than some of the azimuthal reflectivity attributes such as the anisotropic gradient (Rüger, 2002). Further, the inversion provides an unambiguous estimate of the fracture strike. In practice there are a couple of limitations with this approach. First there is no easy way to map layer properties anomalies from the azimuthal elastic inversion to reflectivity attribute anomalies from other methods. Moving back and forth between the layers and reflectivities is important for validation and comparison between various methods. Secondly, we found that there is cross-talk between the isotropic parameter and fracture parameter estimates. This paper makes use of azimuthal Fourier Coefficients (FCs) to address these issues.

Downton et al. (2011) show that azimuthal FCs can be used to separate the amplitude versus offset (AVO) and amplitude versus azimuth (AVAz) problems. This property allows for the separation of the fracture parameter and background isotropic parameter estimation problems. This property is exploited in this paper where instead of using azimuth stacks the azimuthal elastic inversion uses azimuthal FCs as input. By working on azimuthal FCs rather than azimuth stacks it is possible to reduce the cross-talk between the fracture and isotropic background parameter estimates. Further, Downton (2011) showed that azimuthal FCs can be used to obtain an unbiased estimate of the anisotropic gradient and

unambiguous estimate of the fracture strike. In addition, FCs can be used to estimate normal and tangential weaknesses reflectivity parameter estimates. This theory provides a method to link traditional reflectivity attributes such as the anisotropic gradient and the fracture parameters of the azimuthal elastic inversion.

First the azimuthal elastic inversion is reviewed. The cost function is briefly discussed with focus on the misfit term and the limitations of the formulation. Then the azimuthal FCs are presented by illustrating the transformation from azimuthal angle stacks to FCs and their relationship to fracture properties is discussed. Next, the azimuthal elastic inversion is modified to invert FCs by updating the misfit term of the cost function. The benefit of this extension is illustrated on synthetic dataset. A comparison to the near offset Rüger equation is performed on real data where the reconciliation is done through the anisotropic gradient. The advantages of using the layer properties from the azimuthal elastic inversion rather than reflectivities for interpretation are discussed.

Azimuthal elastic inversion

The azimuthal elastic inversion is a model-based approach where angle stacks defined at a variety of azimuths are inverted in order to estimate fracture properties. The inversion assumes a single set of vertical fractures which are parameterized in terms of weaknesses using the linear slip theory (Schoenberg, 1980), Thomsen's parameters (Thomsen, 1986) or Hudson model (Hudson, 1981). All the stacks are inverted simultaneously using a simulated annealing technique to minimize a three-term cost function. The first term is the misfit between the modeled data and the real data expressed as follows:

$$Misfit = \sum_{i,j} \left(\left(R * W - data \right) \left(\theta_i , \phi_j \right) \right)^2 \quad (1)$$

The modeled data is calculated using a convolutional model where the azimuthal reflectivity R is computed using either the full anisotropic Zoeppritz equation (Schoenberg and Protázio, 1992) or some linear approximations (Vavryčuk and Pšenčík, 1998, Pšenčík and Martins, 2001, Shaw and Sen, 2006, …), W is the angle dependent wavelet and *data* is the real azimuthal angle stack. The misfit accounts for all the angles of incidence θ_i and all azimuths Φ_j simultaneously.

The second term of the cost function measures the distance between the prior and current models and controls how far the solution is allowed to move away from the initial trend. For isotropic properties such as P- and S-velocities, the initial model is usually built from the low frequency trend derived from the well logs. It is more complicated for the anisotropic properties where control data is more difficult to obtain. If no well data is available seismically derived information such as the shear-wave splitting and VVAz may be used to help construct the initial fracture/anisotropic model. Alternatively, if no prior information on fractures is available, the initial model is assumed to be isotropic. The third term of the objective function controls the lateral continuity of the estimated parameters. This gives smoothness and stability to the results especially in the presence of noise. The layer-based model combined with the multi-trace algorithm link together cells that are consistent with the stratigraphy.

The theoretical model on which the azimuthal elastic inversion is based is nonlinear and so it is difficult to gain an intuitive understanding of the uncertainty and resolution of each of the parameters. In order to understand the resolution and stability of the parameter estimates we have analyzed the misfit function (Figure 2). The analysis of this is complicated because of the multidimensionality of the problem. In brief we have discovered there is some cross-talk between the background isotropic and fracture parameter estimates. The theoretical basis for this cross-talk can be understood by analyzing the individual azimuthal FCs.

Azimuthal Fourier Coefficients

Downton (2011) described how to transform azimuthal angle stacks into azimuthal FCs. This transformation is illustrated in Figure 1.

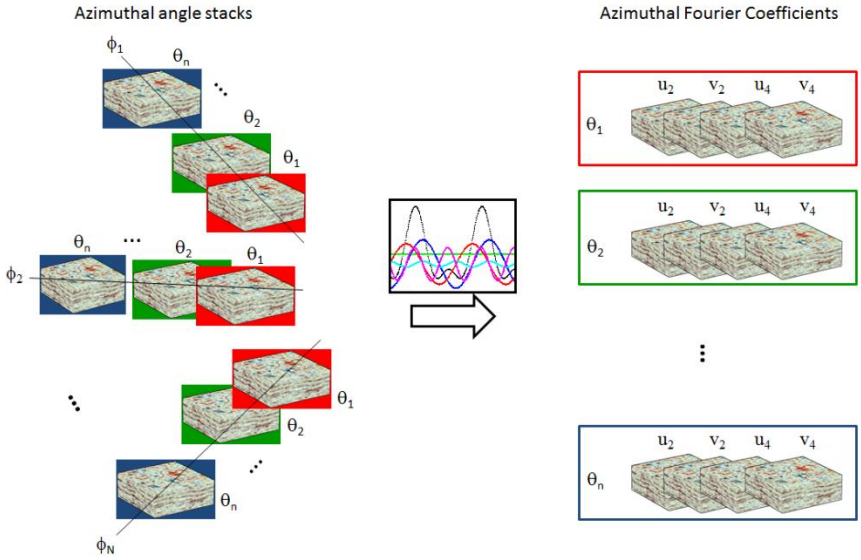

Figure 1: For each angle of incidence, the amplitude variation with azimuth can be decomposed into four FCs by keeping only the 2nd and 4th order terms.

For each angle of incidence, the AVAz signal can be decomposed into FCs. The DC term (order 0) u_0 is the average stack over all the azimuths and contains both the background isotropic reflectivity and the fractures reflectivity (Downton et al., 2011):

$$u_0(\theta) = A + B\sin^2(\theta) + C\sin^2(\theta)\tan^2(\theta) \tag{2}$$

where

$$A = A_{iso} - \frac{1}{4}\chi^2 \Delta\delta_N \tag{3}$$

$$B = B_{iso} + \frac{g}{2}\Delta\delta_T - \frac{\chi}{4}\Delta\delta_N \tag{4}$$

$$C = C_{iso} - \frac{1}{8}g\Delta\delta_T - \frac{1}{8}\left(3g^2 - 4g + 2\right)\Delta\delta_N \tag{5}$$

Equation (2) has the same form as the classic 3-term AVO expression. In this modified form A_{iso}, B_{iso} and C_{iso} are respectively the intercept, gradient and curvature of the background isotropic reflectivity, g is the square of the S-wave to P-wave velocity ratio (Vs/Vp) of the unfractured background rock, $\chi = 1 - 2g$, $\Delta\delta_T$ (resp. $\Delta\delta_N$) is the difference of tangential (resp. normal) weakness between the upper and lower layers. Since u_0 contains both isotropic and fracture properties, it is confusing to invert. Ignoring the fracture properties, we get biased estimates of A, B and C. With the fractures properties, the problem is underdetermined. The fracture and isotropic parameters are linked through equation (2) explaining the cross-talk we are observing in our modeling studies.

For a linearized expression of the azimuthal reflectivity, coefficients of orders greater than 4 can be neglected and due to the reciprocity of PP data, only even orders are non-zero. Consequently, most of the information is contained in the 2nd order cosine (u_2) and sine (v_2) terms and the 4th order cosine (u_4) and sine (v_4) terms. These non-zero FCs are solely a function of the fracture parameters and g. Given g, it is possible to invert the non-zero FCs to estimate the fracture weakness parameters. Once the weaknesses are known, we are then able to get unbiased estimates of A, B and C by solving for u_0.

The fact that g is required still implies that there is a weak coupling between the fracture and background isotropic parameters.

Downton (2011) showed that using one angle of incidence the 2nd FCs correspond to a biased estimate of the anisotropic gradient similar to the one obtained by the near offset Rüger equation. Using multiple angles of incidence, FCs provide an unbiased estimate of the anisotropic gradient and an unambiguous estimate of the fracture strike (the near offset Rüger equation has a 90 degree ambiguity on the orientation of the fractures). We will refer to the method introduced by Downton (2011) as the azimuthal FCs *reflectivity* inversion by opposition to the method presented in this paper which is an azimuthal FCs *elastic* inversion.

Extension of the azimuthal elastic inversion to invert Fourier Coefficients

In order to replace the azimuthal angle stacks by FCs in the azimuthal elastic inversion, the misfit expression of the cost function needs to be updated as follows:

$$Misfit_{FC} = \sum_{i,k} \left(\left(R_{FC}^{k} * W - FC_k \right)(\theta_i) \right)^2 \qquad (6)$$

where R_{FC}^{k} is the reflectivity written using FCs (Downton, 2011) for the u_2 (k=1), v_2 (k=2), u_4 (k=3) and v_4 (k=4) terms. W is the angle dependent wavelet, FC_k is the real k^{th} Fourier Coefficient computed from the azimuthal angle stacks (as illustrated in Figure 1) and θ_i is the angle of incidence. By not including the DC term u_0 in the cost function, the P- and S- impedances and the density reflectivities can be removed from the inversion and we can solve for the fracture problem separately. The benefit of this is illustrated in Figure 2 on synthetic data by comparing the misfit from the azimuthal angle stacks approach to the misfit from the FCs approach.

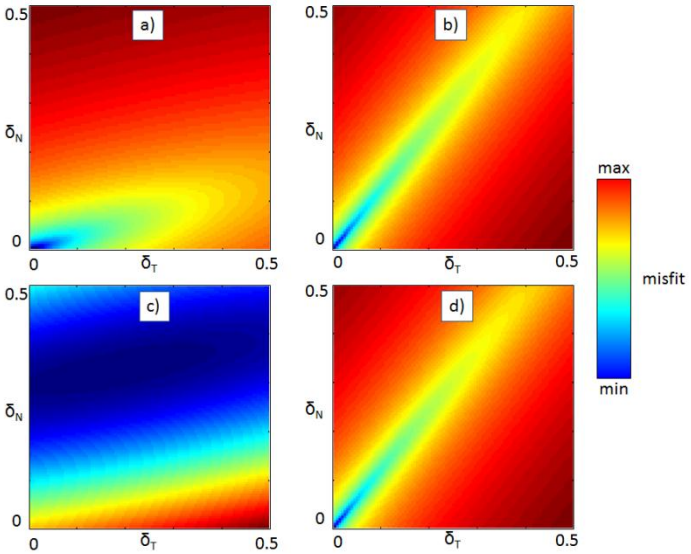

Figure 2: Top: misfit function for isotropic data with *exact* impedances computed using azimuthal angle stacks (a) and FCs (b). The minimum misfit is obtained for (δ_N,δ_T)=(0,0) in both cases. Bottom: misfit function for isotropic data with *biased* impedances computed using azimuthal angle stacks (c) and FCs (d). The minimum misfit is no longer obtained for (δ_N,δ_T)=(0,0) in the case of azimuthal angle stacks.

The synthetic data is isotropic and does not contain any AVAz effect. The isotropic properties are fixed at their exact values and the normal and tangential weaknesses (δ_N and δ_T) are both equal to 0. The global minimum of the misfit will provide the best match between the modeled data and the real rata. The misfit was computed using equations (1) and (6) respectively for the inversion of azimuthal angle stacks and the inversion of FCs. In our example, the misfit exhibits a global minimum at (δ_N,δ_T)=(0,0) for both the azimuthal angle stacks approach (Figure 2a) and the FCs approach (Figure 2b). We then

introduce a bias of about 5% in the impedances and keep them fixed at their biased values. Even though the data is still isotropic, the azimuthal angle stacks approach shows that the minimum misfit moved to non-zero weaknesses values (Figure 2c). Since the reflectivity expression combines both isotropic and anisotropic terms, the bias introduced in the impedances leaked towards the weaknesses and illustrates the cross-talk mentioned previously. By opposition, the misfit of the FCs approach still shows a minimum at (0,0) (Figure 2d) illustrating the benefit of treating the isotropic and fracture problems separately. There is actually a small rotation of the misfit space due to the fact that the inversion of FCs requires a background Vp/Vs ratio, but the fact that it is barely noticeable illustrates the small sensitivity of the inversion with this regards and confirms the weak coupling to the isotropic background mentioned previously.

Comparison between the azimuthal elastic inversion and the near offset Rüger equation

Both the Rüger equation and the azimuthal elastic inversion assume a single set of vertical fractures (HTI). Comparison of the two methods is complicated by the fact that the former is parameterized in terms of interface parameters while the latter is parameterized in terms of layer parameters. In order to compare the two, the layer parameters must be transformed to fractional interface parameters. This can be accomplished by using a modified form of the anisotropic gradient given by Bakulin et al. (2000):

$$B_{ani} = g\left(\Delta\delta_T - (1-2g)\Delta\delta_N\right) \qquad (7)$$

where B_{ani} is the anisotropic gradient, g is the square of the background S-wave to P-wave velocity ratio and $\Delta\delta_T$ (resp. $\Delta\delta_N$) is the difference of tangential (resp. normal) weakness between the upper and lower layers. We then need to convolve B_{ani} with a wavelet in order to compare with the band-limited near offset Rüger equation results. Figure 3 shows such a comparison.

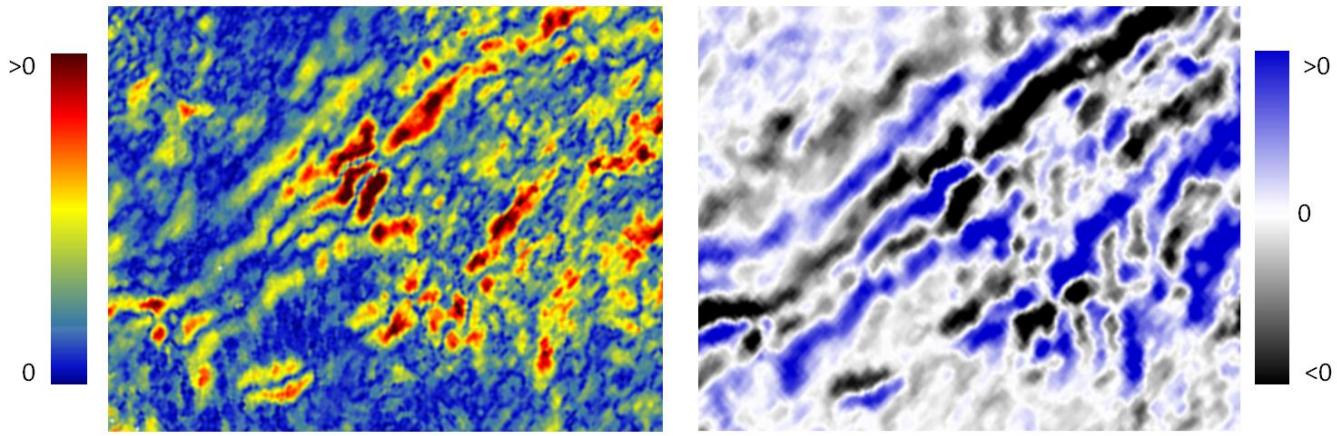

Figure 3: Time slice of a Western Canadian 3D showing the anisotropic gradient B_{ani} computed using the near offset Rüger equation (left) and the azimuthal elastic inversion (right). Removing the restriction on the sign of B_{ani} and using a more theoretically correct model results in a clearer image of the fractures.

The anisotropic gradient computed using the near offset Rüger equation (Figure 3, left) is limited to positive values due to solving for the magnitude. However there is no restriction on the sign of the anisotropic gradient from the azimuthal elastic inversion (Figure 3, right) and it seems to better identify a strike slip fault known in the area (close to the diagonal from the top right to the bottom left corners). The azimuthal inversion shows more continuity and more robustness to the noise due to extra stability brought by coupling the layers. Also the model used is more theoretically correct as it is a far angle formulation that allows the symmetry axis to change with layers.

Figure 4 shows the results obtained for the symmetry axis (direction perpendicular to the fracture strike) on a horizon slice from the same dataset.

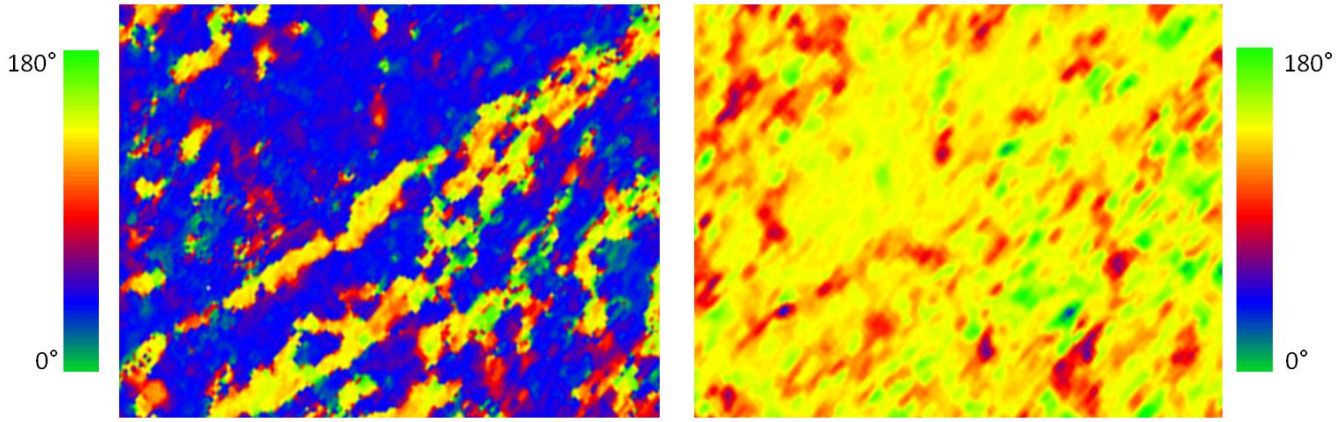

Figure 4: Real dataset example of symmetry axis computed using the near offset Rüger equation (left) and the azimuthal elastic inversion (right). The direction obtained with the azimuthal elastic inversion is consistent with the dominant stress (135°) though the near offset Rüger equation shows an error of 90 degrees outside the fault.

The ambiguity from the near offset Rüger formulation appears as a 90 degree error outside the fault area whereas the symmetry axis from the azimuthal inversion is consistent with the dominant stress in the area (135°). The deviations observed from the main trend are due to zones of small anisotropy or isotropy in which case the symmetry axis is not meaningful.

Interpretation

The interpretation of B_{ani} is not as straightforward as the interpretation of the weakness parameters. Assuming Hudson theory, it is possible to relate B_{ani} to the fracture intensity. But it is actually a weighted difference between δ_T and δ_N (see equation (7)) and it is possible for these parameters to annihilate each other (Goodway, 2006). For dry fractures and still assuming Hudson theory, there is a typical Vs/Vp ratio value close to 0.55 where B_{ani} becomes 0 (Bakulin et al., 2000). Also, B_{ani} is an interface property and consequently more complicated to interpret than interval properties. The interval weaknesses provided by the azimuthal elastic inversion are more straightforward to interpret. Both weaknesses are a function of the fracture intensity and δ_N has a fluid sensitivity if Hudson theory is assumed and both weaknesses can be related to Thomsen's parameters.

Figure 5 shows how the interface property B_{ani} (left) and the layer property δ_T (right) visually relate to each other for a particular horizon of a 3D Canadian dataset. In that case a strike slip fault is identified by large weakness values corresponding to large positive B_{ani} values. δ_T appears to be a good indicator.

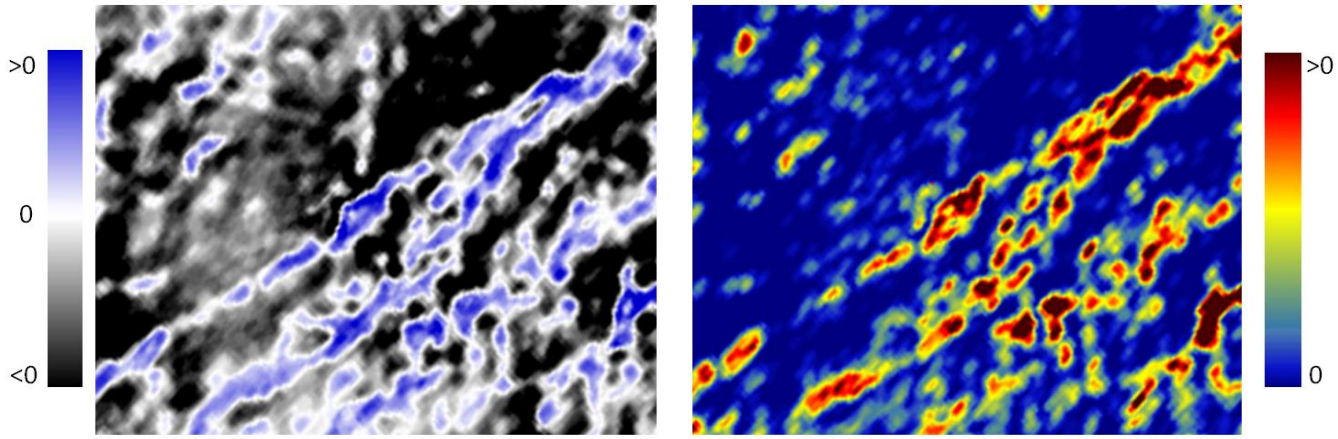

Figure 5: Horizon slice of a real Canadian dataset. Left: anisotropic gradient B_{ani} and right: tangential weakness δ_T both estimated with the azimuthal elastic inversion. Large positive B_{ani} correspond to large δ_T with the benefit that δ_T is an interval property so easier to relate to the geology.

In the future, more research will help understand fractures through the weaknesses. For example, Perez (2010) proposed a method to interpret the weaknesses using the LMR cross-plot, Close et al. (2011) used the azimuthal elastic inversion to estimate the closure stress and Perez et al. (2011) mentioned the benefits of using fracture information for interpretation.

Discussion

The differences between the azimuthal FCs *elastic* inversion we present here and the azimuthal FCs *reflectivity* inversion introduced by Downton (2011) is analog to the differences between the isotropic elastic inversion and the AVO reflectivity inversion. Elastic inversion is more stable than reflectivity inversion due to the coupling between the layers (see Figure 6) but it requires a more involved workflow (wavelet estimation, initial model building, inversion parameters tuning …). Seismic gives us interface parameters but layers are easier to interpret. Both methods can be reconciled using the anisotropic gradient but future work will involve reconciling them through the weaknesses.

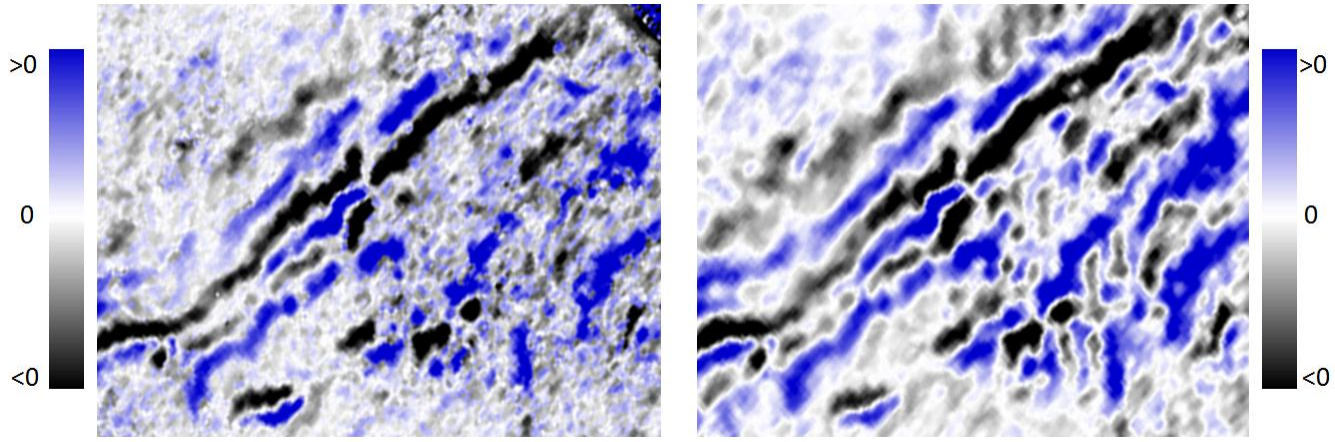

Figure 6: Time slice of a real Canadian dataset. Anisotropic gradient estimated from the azimuthal FCs reflectivity (left) and elastic (right) inversions. The coupling between the layers brings stability to the elastic inversion but the drawback is that a more involved workflow is required.

Also, more complex models could be used to remove some of the inversion assumptions. For example the tangential weakness δ_T could be decomposed in vertical weakness δ_V and horizontal weakness δ_H (Shaw and Sen, 2006) to allow more general forms of crack but it means inverting an extra parameter and raises the issue of stability.

Conclusions

The extension of the azimuthal elastic inversion to invert Fourier Coefficients stabilizes the process by treating the fracture properties separately from the isotropic background properties. This decoupling reduces the number of properties to invert for and avoids leakage due to cross-talk between the estimates. The azimuthal Fourier Coefficient elastic inversion outputs can easily be converted to reflectivity data, e.g. the commonly used anisotropic gradient, for comparison with other methods and shows less ambiguous results than the near offset Rüger equation. The elastic inversion shows a better signal-to-noise characterization than reflectivity methods, but requires a more involved workflow. Lastly, the azimuthal elastic inversion outputs layer properties such as the fracture weaknesses that will help in the interpretation and understanding of fractures.

Acknowledgements

The authors thank Apache and EnCana for permission to show the data. We thank Bill Goodway, Marco Perez and Dave Close for stimulating discussions that helped us in this line of research. We also thank Yves Lafet and Jean-Philippe Coulon for the support they gave in preparing this work.

References

Bakulin, A., V. Grechka, and I. Tsvankin, 2000, Estimation of fracture parameters from reflection seismic data - Part I: HTI model due to a single fracture set: Geophysics, **65**, 1788-1802.

Close, D. I., M. Perez, B. Goodway, F. Caycedo, and D. Monk, 2011, Workflows for Integrated Seismic Interpretation of Rock Properties and Geomechanical Data: Part 2 – Application and Interpretation: CSEG, Expanded Abstracts.

Coulon, J.-P., Y. Lafet, B. Deschizeaux, P. M. Doyen, and P. Duboz, 2006, Stratigraphic elastic inversion for seismic lithology discrimination in a turbiditic reservoir: SEG, Expanded Abstracts.

Downton, J., 2011, Azimuthal Fourier Coefficients: a simple method to estimate fracture parameters: SEG, Expanded Abstracts.

Downton, J., and B. Roure, 2010, Azimuthal simultaneous elastic inversion for fracture detection: SEG, Expanded Abstracts.

Downton, J., B. Roure, and L. Hunt, 2011, Azimuthal Fourier Coefficients: CSEG Recorder, **36**, no. 10, 22-36.

Goodway, B., J. Varsek, and C. Abaco, 2006, Practical applications of P-wave AVO for unconventional gas Resource Plays, Part II: Detection for fracture prone zones with Azimuthal AVO and coherence discontinuity: CSEG Recorder, **31**, no. 4, 52-65.

Hudson, J. A., 1981, Wave speeds and attenuation of elastic waves in material containing cracks: Geophysical Journal of the Royal Astronomical Society, **64**, 133-150.

Perez, M., 2010, Beyond Isotropy – Part II: Physical Models in LMR space: CSEG Recorder, **35**, no. 8, 36-43.

Perez, M., D. I. Close, B. Goodway, and G. Purdue, 2011, Developing Templates for Integrating Quantitative Geophysics and Hydraulic Fracture Completions Data: Part I - Principles and Theory: SEG, Expanded Abstracts, 1794-1798.

Pšenčík, I., and J. L. Martins, 2001, Properties of weak contrast PP reflection/transmission coefficients for weakly anisotropic elastic media: Studia Geophysica et Geodaetica, **45**, 176-197.

Rüger, A., 2002, Reflection coefficients and azimuthal AVO Analysis in anisotropic media: SEG geophysical monograph series number 10.

Shaw, R. K., and M. K. Sen, 2006, Use of AVOA data to estimate fluid indicator in a vertically fractured medium: Geophysics, **71**, C15.

Schoenberg, M., and J. Protázio, 1992, Zoeppritz rationalized and generalized to anisotropy: Journal of Seismic Exploration, **1**, 125-144.

Schoenberg, M., 1980, Elastic behaviour across linear slip interfaces: Journal of the Acoustical Society of America, **68**, no. 5, 1516–1521.

Thomsen, L., 1986, Weak elastic anisotropy: Geophysics, **51**, 1954-1966.

Vavryčuk, V., and I. Pšenčík, 1998, PP-wave reflection coefficients in weakly anisotropic elastic media: Geophysics, **63**, 2129-2141.